Structural stability of thallium–V compounds

2007 J. Phys.: Condens. Matter 19 106221

(http://iopscience.iop.org/0953-8984/19/10/106221)

IOP PUBLISHING JOURNAL OF PHYSICS: CONDENSED MATTER

J. Phys.: Condens. Matter **19** (2007) 106221 (18pp) doi:10.1088/0953-8984/19/10/106221

Structural stability of thallium–V compounds

Nawal Saidi-Houat[1,2], Ali Zaoui[3] and Mohamed Ferhat[1]

[1] Département de Physique, Université des Sciences et de la Technologie d'Oran, Oran, USTO, Algeria
[2] Faculté des Sciences, Université de Mostaganem, Mostaganem, Algeria
[3] LML, Polytech'Lille, Université des Sciences et de la Technologie de Lille, Cité Scientifique, Avenue Paul Langevin, 59655 Villeneuve D'Ascq Cedex, France

Received 8 December 2006, in final form 22 January 2007
Published 23 February 2007
Online at stacks.iop.org/JPhysCM/19/106221

Abstract

We have performed *ab initio* self-consistent calculations in order to investigate the structural stability of the thallium–V compounds: TlN, TlP, TlAs, TlSb and TlBi. Total energy calculations of several phases are considered here in order to fix the most stable structure for each compound. For the structures considered, the wurtzite one is found to be the ground state phase for TlN, the zinc-blende phase that for TlP and TlAs, while TlSb and TlBi favour the tetragonal PbO phase. Some unusual features, compared with the other III–V families, are registered for the systems studied, which we attempt to analyse and to explain in detail in the present paper.

(Some figures in this article are in colour only in the electronic version)

1. Introduction

Recently, it has been suggested that optoelectronic devices based on thallium–V have advantages over the II–VI semiconductor devices, as an alternative to HgCdTe, for interesting applications in optical communication systems (laser diodes, detectors) in the near-infrared wavelength region. The earlier pioneering theoretical works of Van Schilfgaarde *et al* [1, 2] and Krishnamurthy *et al* [3] on TlInP, TlInAs, and TlInSb and the improvements of the epitaxial growth technology, such as for the metal–organic vapour phase epitaxy (MOVPE) and the molecular-beam epitaxy (MBE), have opened the way to study of the growth and the electronic properties of III–V compounds containing thallium.

It is expected that the most Tl–V compounds should have a small or even negative gap. Combination of Tl with III–V compounds yields interesting new III–V semiconductor alloys, containing semiconductor and semi-metal compounds; for example $In_{1-x}Tl_xP$ would have a lattice constant essentially equal to that of InP, and a band gap ranging from the 1.3 eV band gap of InP down to 0 eV with increasing thallium content. The idea is essentially that Tl could be substituted for In with little change in lattice constant and a significant decrease in band gap, thus extending the range of band gaps available for materials lattice matched to

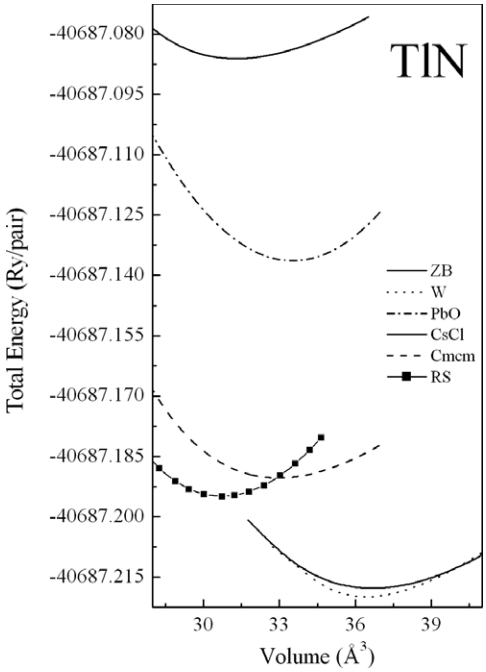

Figure 1. Total energy versus volume for the zinc-blende (ZB), wurtzite (W), rock-salt (NaCl), CsCl and *Cmcm* phases of TlN.

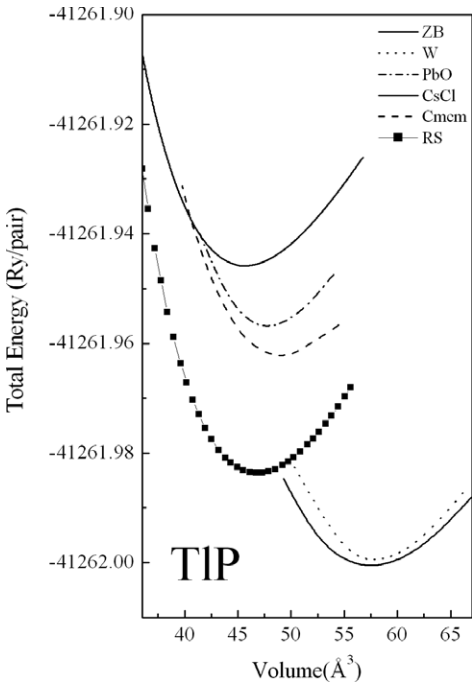

Figure 2. Total energy versus volume for the zinc-blende (ZB), wurtzite (W), rock-salt (NaCl), CsCl and *Cmcm* phases of TlP.

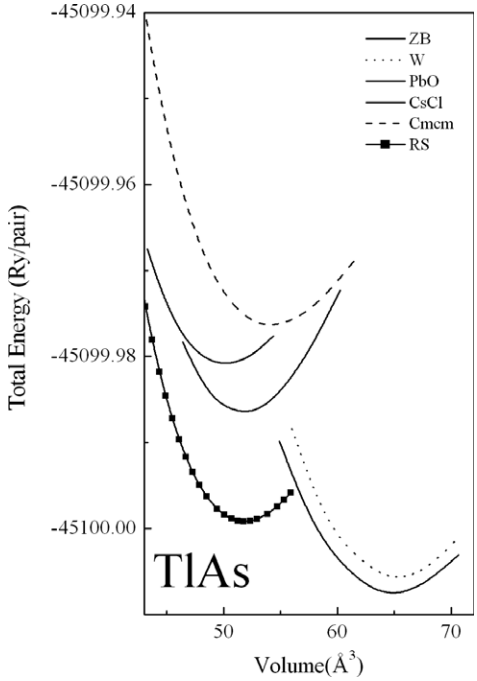

Figure 3. Total energy versus volume for the zinc-blende (ZB), wurtzite (W), rock-salt (NaCl), CsCl and *Cmcm* phases of TlAs.

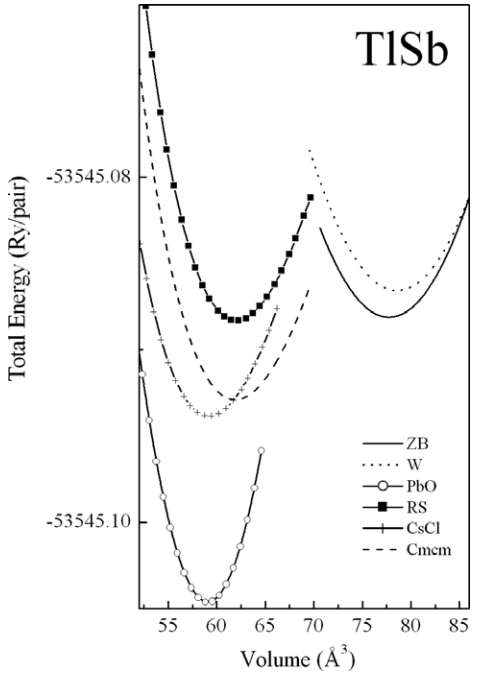

Figure 4. Total energy versus volume for the zinc-blende (ZB), wurtzite (W), rock-salt (NaCl), CsCl and *Cmcm* phases of TlSb.

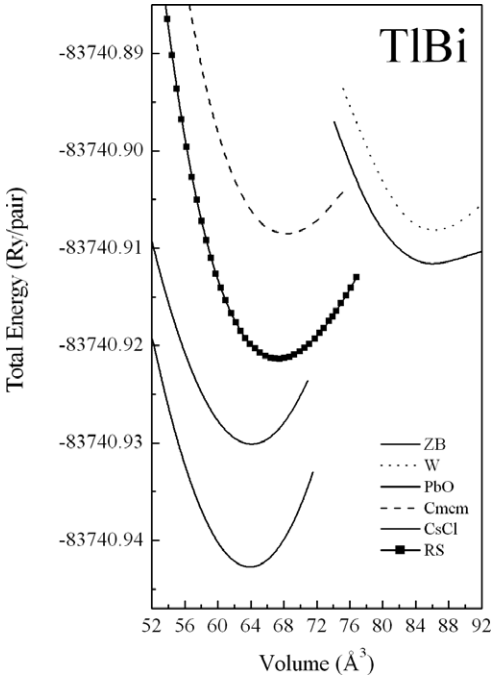

Figure 5. Total energy versus volume for the zinc-blende (ZB), wurtzite (W), rock-salt (NaCl), CsCl and *Cmcm* phases of TlBi.

Table 1. Calculated structural parameters for Tl–V compounds. In parentheses, we give the ground state phase.

		a (Å)	c (Å)	u	B_0 (GPa)
TlN(W)	Present calculation	3.746	6.014	0.372	112.67
	Other calculation[a]	3.766	5.768		
		a (Å)			B_0 (GPa)
TlP(ZB)	Present calculation	6.124			46.75
	Other calculation	5.747[b], 5.96[c]			71.30[b], 57[c]
TlAs(ZB)	Present calculation	6.382			44.37
	Other calculation	5.946[b], 6.18[c], 6.27[d]			58.90[a], 49[b]
		a (Å)	c (Å)	z	B_0 (GPa)
TlSb(PbO)	Present calculation	4.650	5.473	0.499	67.08
TlBi(PbO)	Present calculation	4.903	5.327	0.499	61.43

[a] Reference [17].
[b] Reference [18].
[c] Reference [2].
[d] Reference [19].

GaAs and InP. Therefore Tl–(III–V) alloys [4–12] are strong potential candidate materials for novel infrared detector use. However, less is known about the ground state structure of the thallium–V groups. The structural parameters, electronic properties, and ground state structure of the Tl–V compounds are unfortunately still not known. Since the knowledge of the stability of these compounds in conjunction with their electronic properties is critical for a promoting

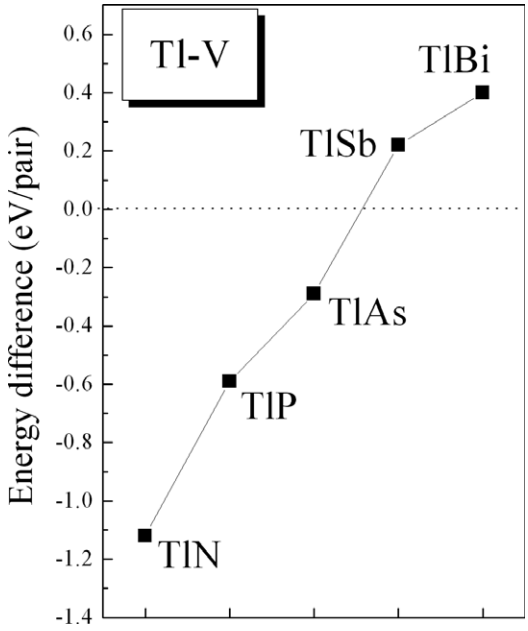

Figure 6. Total energy difference between ZB and PbO phases for the Tl–V group.

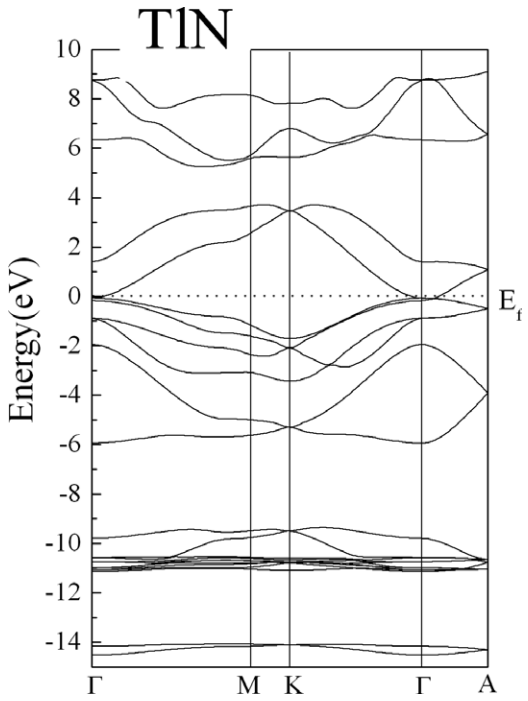

Figure 7. Calculated band structure of TlN in the wurtzite phase.

alloy, a detailed theoretical study is necessary. In this paper we present a systematic predictive study of the structural and electronic properties of Tl–V by using the state of the art *ab initio*

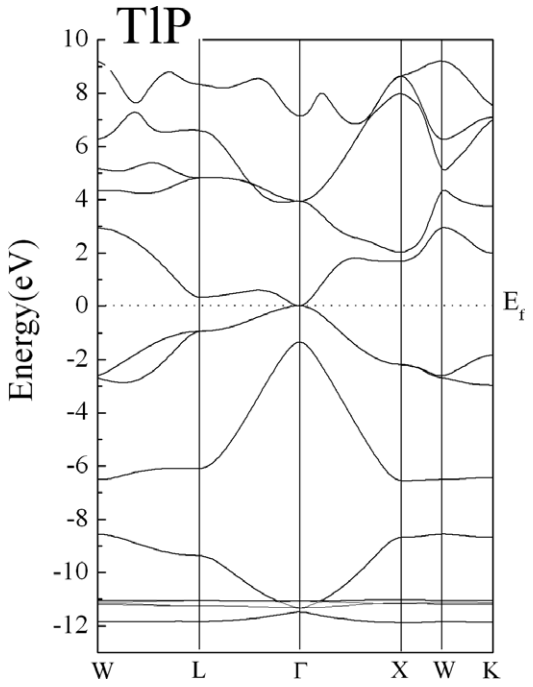

Figure 8. Calculated band structure of TlP in the zinc-blende phase.

self-consistent full potential linearized augmented plane wave (FPLAPW) approach. The rest of the paper is organized as follows. In section 2, we briefly describe the computational method used in the present work. Results for the structural and electronic properties will be presented in section 3. A summary of the work will be given in section 4.

2. Method

The calculations were performed in the framework of density functional theory, DFT. We have employed the full potential linearized augmented plane wave (FLAPW) method as implemented in the WIEN2k code [13]. The exchange and correlation effects were treated using the generalized gradient approximation (GGA) [14]. We expand the basis function up to $R_{\mathrm{MT}}K_{\mathrm{MAX}} = 8$ (R_{MT} is the plane wave radius, K_{MAX} is the maximum modulus for the reciprocal lattice vectors). The maximum value for partial waves inside the atomic sphere is $l = 10$. Fully relativistic approximation is used for core electrons, and scalar relativistic approximations are used for valence electrons. Accurate Brillouin zone integrations are performed using the standard special k points technique of Monkhorst and Pack (MP) [15]. For the zinc-blende (ZB) and wurtzite (W) phases, we have used $9 \times 9 \times 9$ and $9 \times 9 \times 4$ MP meshes respectively. For the caesium chloride (CsCl) phase we have used $10 \times 10 \times 10$ MP meshes, for the $Cmcm$ phase we have used $7 \times 7 \times 4$ MP meshes, and for the rock-salt (NaCl) phase we have used $11 \times 11 \times 11$ MP meshes. The corresponding integrating points over the irreducible Brillouin zone are 56 k points for CsCl and NaCl phases, 55 k points for the ZB phase, and 48 k points for the W and the $Cmcm$ phases. We carefully checked that these computational parameters were sufficient for accurately determining total energies within 0.5–1 meV per cell.

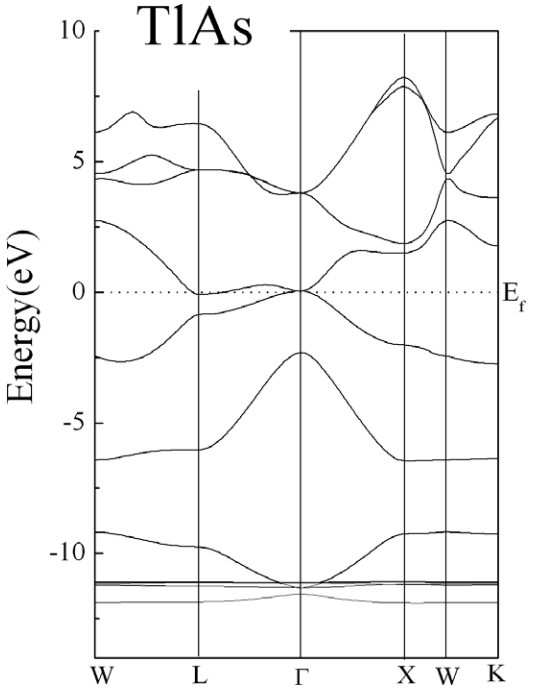

Figure 9. Calculated band structure of TlAs in the zinc-blende phase.

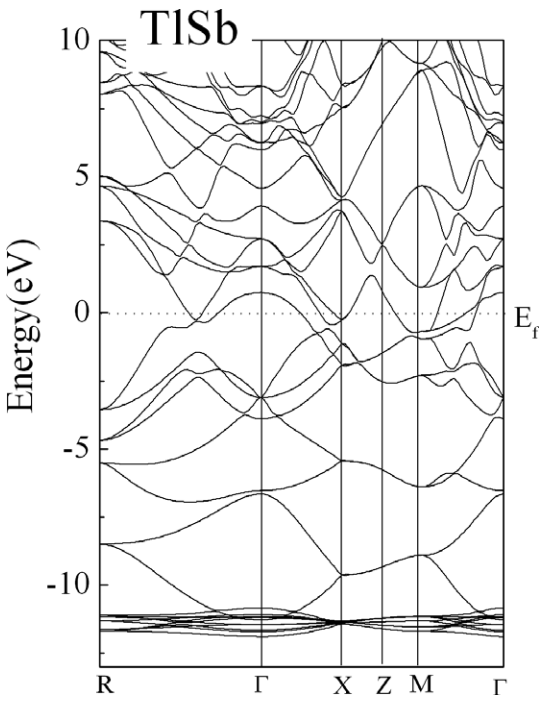

Figure 10. Calculated band structure of TlSb in the PbO phase.

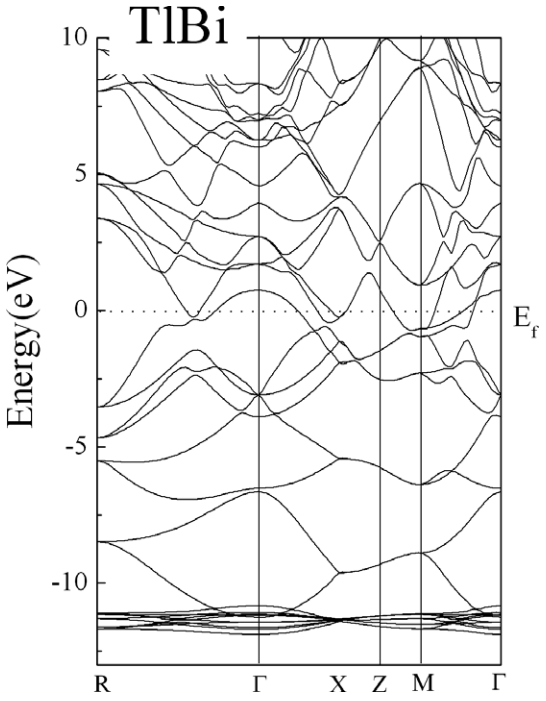

Figure 11. Calculated band structure of TlBi in the PbO phase.

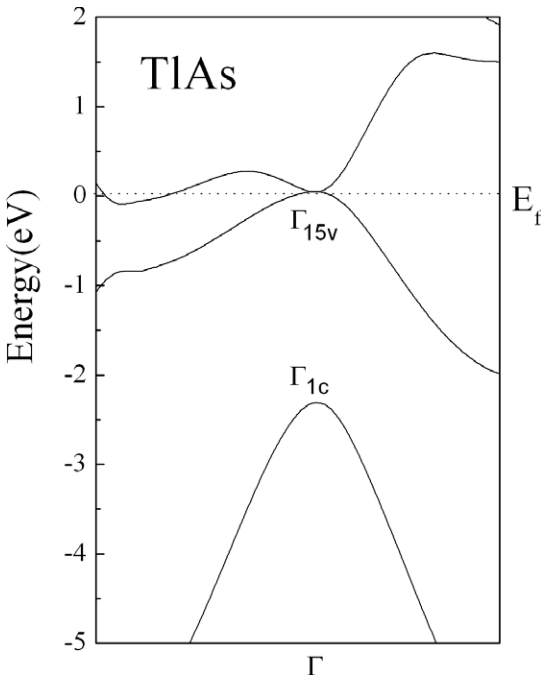

Figure 12. Calculated band structure of TlAs in the zinc-blende structure, between −5 and 2 eV.

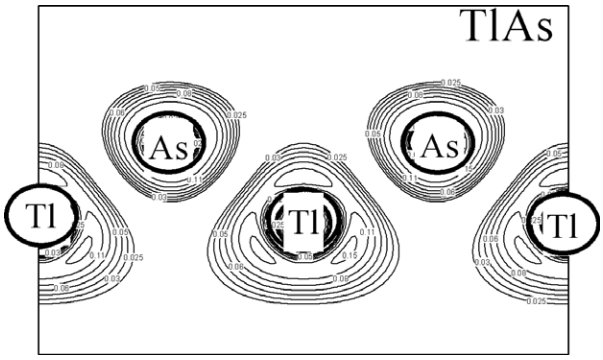

Figure 13. Charge density plot for the Γ_{1c} state of TlAs.

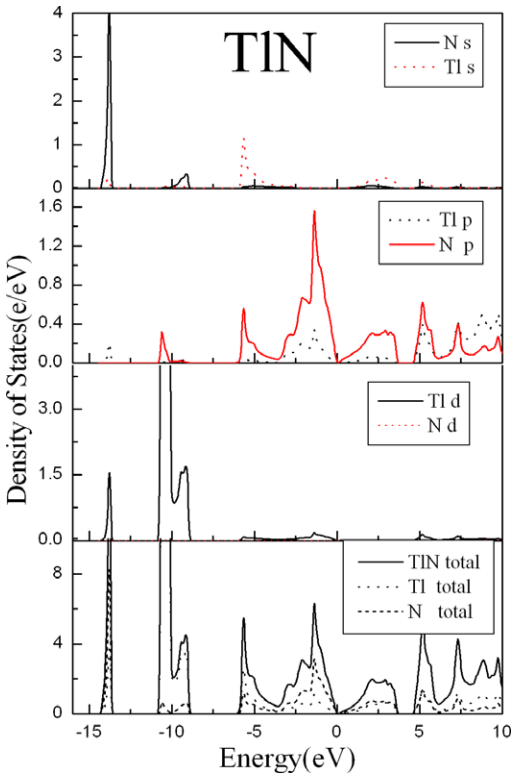

Figure 14. Total and partial densities of states of TlN.

3. Results and discussion

Total energy versus volume data for the zinc-blende, wurtzite, rock-salt, CsCl, *Cmcm* phases and tetragonal (PbO) are shown in figures 1–5 for the Tl–V compounds. The calculated total energies are fitted with Murnaghan's equation of state [16] to obtain structural parameters. The calculated structural parameters for the ground state phase are given in table 1. The calculated lattice parameters and bulk modulus are, in general, in favourable agreement with the previous calculations; however there is no experimental result available for the Tl–V compounds.

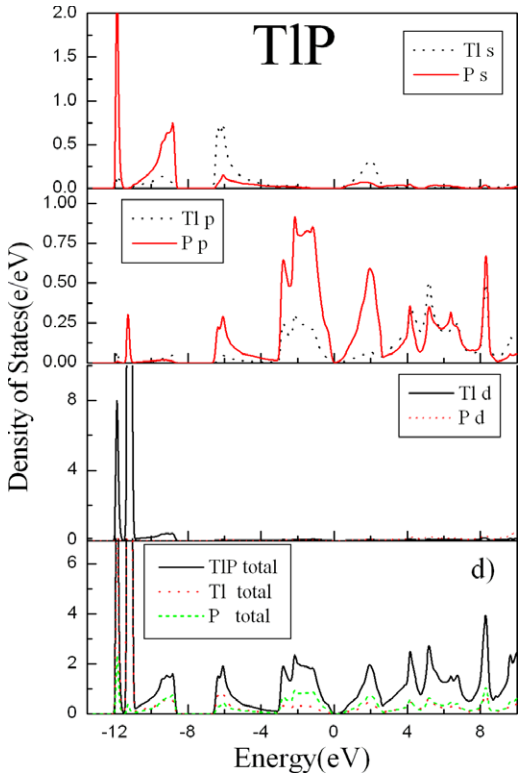

Figure 15. Total and partial densities of states of TlP.

Table 2. Stable crystal structure of III–V compounds.

	N	P	As	Sb	Bi
B	Graphite	ZB	ZB	ZB	ZB
Al	W	ZB	ZB	ZB	ZB
Ga	W	ZB	ZB	ZB	ZB
In	W	ZB	ZB	ZB	PbO
Tl	W	ZB	ZB	PbO	PbO

We find that the wurtzite structure is the most stable structure for TlN as found for other III–V nitrides. For TlAs and TlP, we found that the zinc-blende phase is the ground state structure. However, for the heavier compounds TlSb and TlBi, we found that the tetragonal (PbO) phase is the preferred one. Similar results were found previously for the heavier III–Bi [20], where the only synthesized compound, InBi, has been found as stable in the PbO tetragonal structure [21]. The PbO structure is a likely candidate for showing structural ground state stability for the heavy Tl–V compounds: TlSb and TlBi.

In figure 6, we present the total energy difference ($\Delta E_{\mathrm{ZB-PbO}}$) between the ZB and the PbO phases for the Tl–V group. The total energy difference increases as the anion becomes heavier (i.e., from TlN to TlBi). Hence, the PbO phase is stabilized over the wurtzite and the zinc-blende phases as the Tl–V compounds become heavier.

As shown previously [22] (table 2), we have now a clear picture of the phase stability of all III–V compounds; column III nitrides adopt the W structure, and the other heavier column III

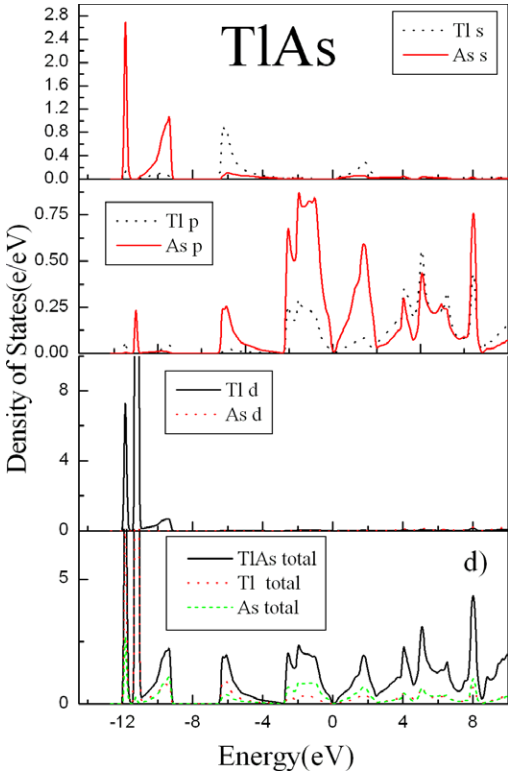

Figure 16. Total and partial densities of states of TlAs.

Table 3. Calculated s and p level energies (eV) of Tl, and V elements.

	E_s (eV), relativistic	E_s (eV), non-relativistic	E_p (eV), relativistic	E_p (eV), non-relativistic
N	−19.86	−19.84	−8.31	−8.30
P	−14.78	−14.71	−6.31	−6.28
As	−15.91	−14.77	−6.1	−5.94
Sb	−13.97	−12.50	−5.87	−5.52
Bi	−13.57	−11.03	−5.22	−4.40
Tl	−9.34	−7.17	−3.1	−2.81

anions favour the zinc-blende structure; whereas the heavier Tl–V (TlSb, and TlBi) and III–Bi (InBi) stabilize in the tetragonal PbO structure.

The calculated relativistic band structures for TlN, TlP, TlAs, TlSb,and TlBi in their ground state phases are shown in figures 7–11 respectively. All compounds show a negative band gap. However, it is well known that the energy band gaps are not given accurately by the GGA because it does not truly represent quasi-particle excitation energies. The energy of the s-like Γ_c state, which is the conduction band minimum (CBM) at the Γ point, is below the p-like valence band maximum (VBM) Γ_v, because the conduction state Γ_{1c} is below the valence state Γ_{15v} (e.g., TlAs; figure 12). These materials are called 'negative band gap' materials. This inversion is caused by the fact that the concave upwards conduction band has dropped in energy and become concave downwards, and it is now occupied (e.g., TlAs; figure 13).

Table 3 gives the calculated s and p energy with and without relativistic effects for N, As, P, As, Sb, Bi, and Tl. Table 3 shows that the relativistic effect significantly lowers the s orbital

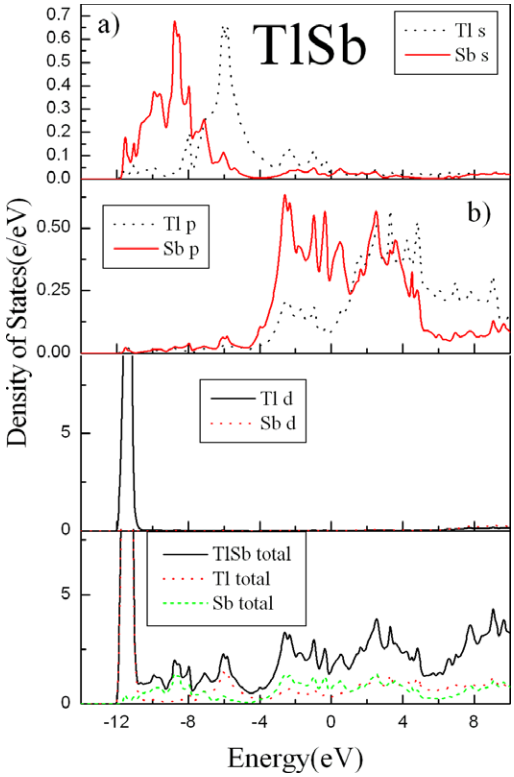

Figure 17. Total and partial densities of states of TlSb.

as the atomic mass increases (e.g., from N → Tl, Bi), while the p orbitals are affected to a lesser extent. For the superheavy atoms of groups III and V, the contractions of the s orbital are strong, and lower considerably the energy of the 6s orbitals of Tl and Bi, by 2.17 and 2.54 eV respectively. Hence the relativistic effects reduce considerably the band gaps of the thallium–V group; this reduction is amplified for TlSb and TlBi. Such a situation exists for common III–V compounds, but with relatively weak relativistic effects for InAs, InSb and GaSb with small band gaps [23] of 0.417, 0.2135 and 0.812 eV respectively.

Figures 14–18 show the calculated total and partial density of states for TlN, TlP, TlAs, TlSb and TlBi respectively. The lowest valence bands are derived essentially from the s electrons of the anion. The lowest valence bands around −12 eV are entirely derived from the d electrons of Tl, while the highest valence bands are derived essentially from the anion p orbitals, with a weak contribution of the p orbitals of Tl. The highest valence bands are characterized exclusively by the contributions of the p orbitals of Tl and anion atoms.

The calculated densities of states of thallium–V compounds show features that differ considerably from those of typical III–V compounds. In particular we found two anion s-like peaks at the bottom of the valence bands; this feature is more apparent for TlP and TlAs (see figures 15(d) and 16(d)). However, except GaN and InN [24], most III–V semiconductors have a single anion-like state near the bottom of the valence band (e.g., GaP; figure 19(c)). The existence of the split-off second anion s-like state is a consequence of the weak separation between s and d bands leading to a strong s–d coupling. In addition to the unusual split-off second anion s states, we found that the lowest valence bands of Tl–V compounds have

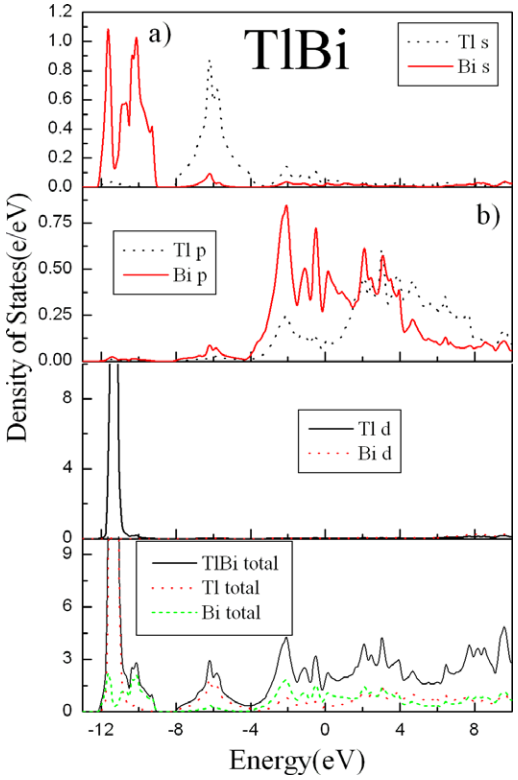

Figure 18. Total and partial densities of states of TlBi.

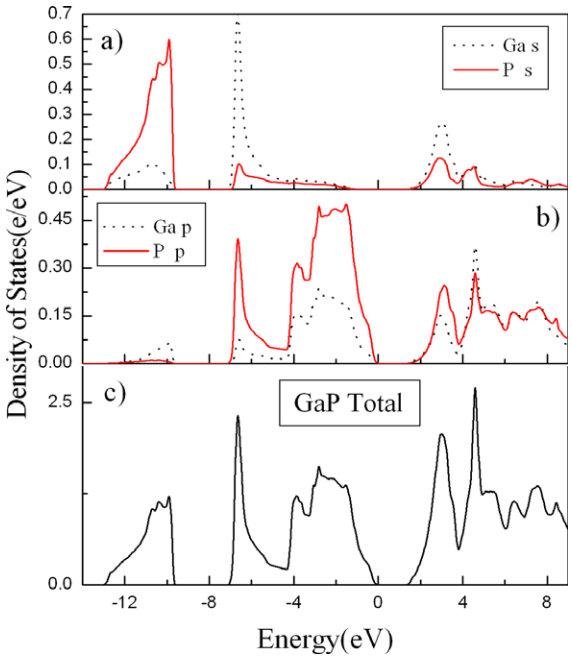

Figure 19. Total and partial densities of states of GaP.

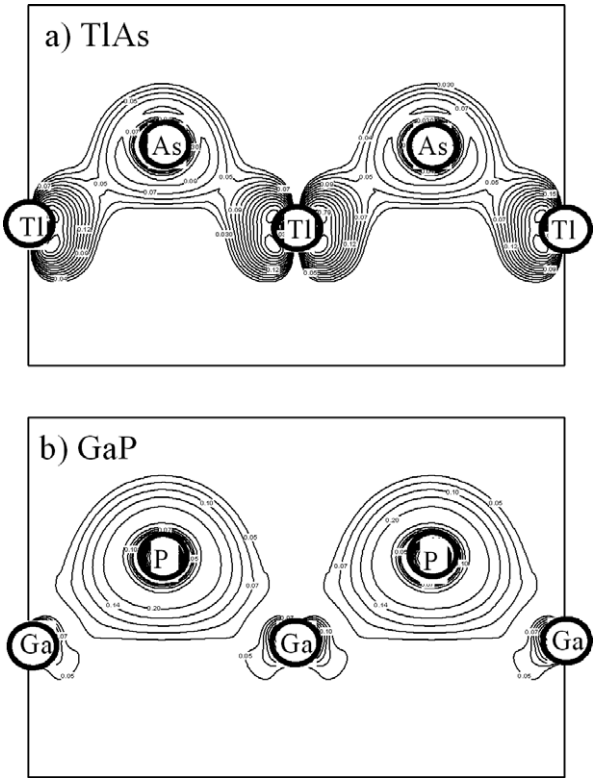

Figure 20. Charge density plot for the Γ_{1V} state of TlAs (a) and GaP (b).

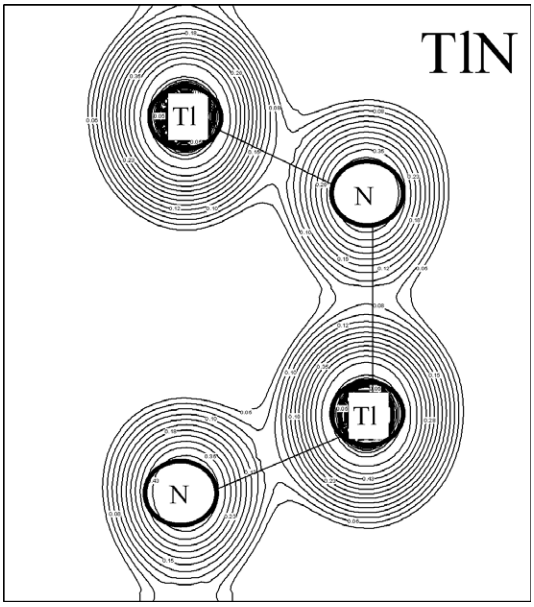

Figure 21. Total valence charge density plot for TlN.

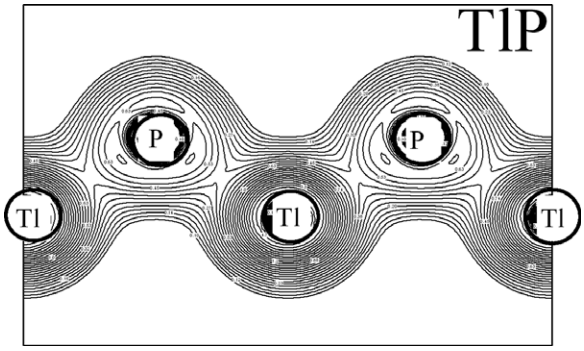

Figure 22. Total valence charge density plot for TlP.

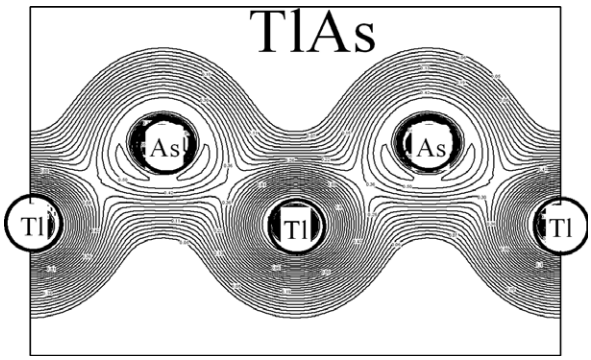

Figure 23. Total valence charge density plot for TlAs.

s (anion) and strong d (cation) Tl character (e.g., TlAs; figure 20(a)); whereas common III–V compounds show strong anion s states (e.g., GaP; figure 20(b)).

The consequence of the relativistic effects in lowering the s level of Tl can be appreciated by inspecting the calculated atom-projected s band densities of states (figures 17(a) and 18(a)) of TlSb and TlBi. Indeed, from figures 17(a) and 18(a) we may see that the s levels of Tl(Sb, Bi) are close to the bottom of the valence bands, and are absent in the conduction bands, whereas III–V compounds show appreciable antibonding s bands in the conduction bands (e.g., GaP; figure 19(a)). Finally while the p bands of III–V compounds (e.g., GaP; figure 19(b)) are clearly distinct in valence (bonding state) and conduction (antibonding state) bands, the Tl–V compounds show strong spatially extended anion and cation p bands around the Fermi level (e.g., TlSb, and TlBi; figures 17(b), 18(b)).

To complete the entire basic background of thallium–V compounds, let us investigate their bonding properties. We show in figures 21–25 the valence charge density distributions of TlN, TlP, TlAs, TlSb, and TlBi respectively. The charge distributions show spherical concentration centred on the Tl and heavier anion atoms Sb and Bi. The d orbital of Tl, Sb and Bi makes up the most of this charge. While in TlN, we notice a relatively strong charge transfer from the N to the Tl atom, this charge transfer decreases rapidly in going from N to Bi (e.g., TlN $\rightarrow$ TlBi). The analysis of the charge density around the Fermi level for TlAs as a prototype of Tl–V compounds shows a relatively weak (strong) bonding (antibonding) state (figure 26(a)) relative to the common III–V compound GaP which shows strong anion and cation p bonding states at the Fermi level (figure 26(b)). While TlN, TlP and TlAs are characterized by a relatively

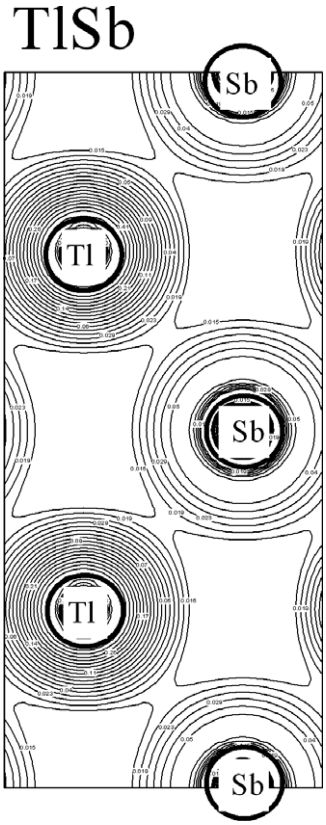

Figure 24. Total valence charge density plot for TlSb.

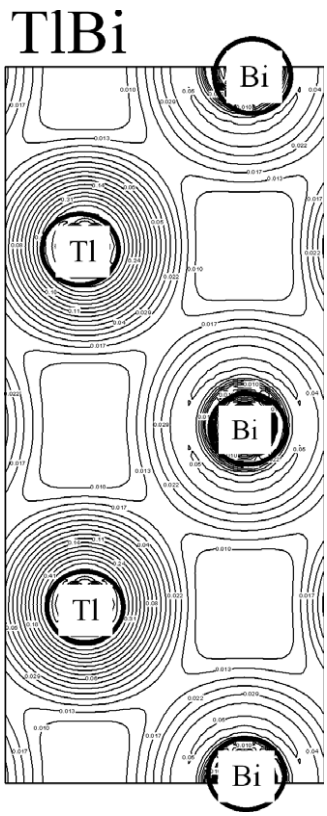

Figure 25. Total valence charge density plot for TlBi.

ionic bonding, the other heavier thallium compounds TlSb and TlBi show a weak bonding; the charge density shows a homogeneous distribution and consequently can be considered as the result of metallic bonding.

4. Summary

We have performed *ab initio* self-consistent calculations using the full potential linear augmented plane wave method to investigate the structural and the electronic properties of the less known thallium III–V compounds: TlN, TlP, TlAs, TlSb and TlBi. Total energy calculations for the cubic zinc-blende, wurtzite, rock-salt, caesium chloride and orthorhombic *Cmcm* phases are investigated. Ground state parameters are computed, and compared with available theoretical works. Among the structures considered, the wurtzite one is found to be the ground state phase of TlN, and the zinc-blende phase is found to be the ground state of TlP and TlAs, while TlSb and TlBi favour the tetragonal PbO structure. The calculated electronic properties of thallium–V compounds show features that differ considerably from those of the other typical III–V semiconductors. In particular we found an inverted band gap, which reflects the semi-metallic character of these systems. We found two anion s-like peaks in the bottom of the valence band, due to a strong s–d coupling. In addition the lowest valence band of thallium compounds shows a strong thallium d character. Finally, we have analysed their bonding nature

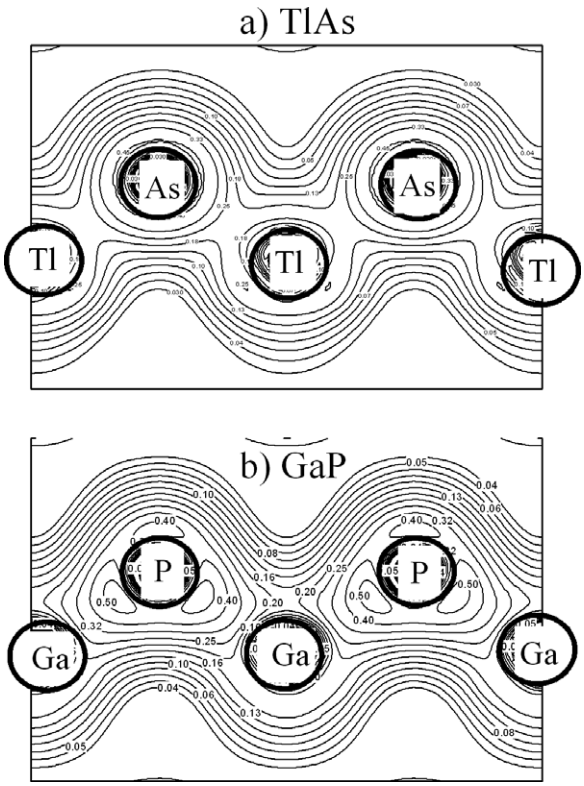

Figure 26. Total charge density plot at the Fermi level of TlAs (a) and GaP (b).

in terms of valence charge density, which shows a gradual increase (decrease) in metallic (ionic) bonds.

References

[1] Van Schilfgaarde M, Chen A-B and Sher A 1992 *Appl. Phys. Lett.* **62** 1857
[2] Van Schilfgaarde M, Chen A-B, Krishnamurthy S and Sher A 1994 *Appl. Phys. Lett.* **65** 2714
[3] Krishnamurthy S, Chen A-B and Sher A 1996 *Appl. Phys. Lett.* **80** 4045
[4] Choi Y H, Besikci C, Sudharsanan R and Razeghi M 1993 *Appl. Phys. Lett.* **63** 361
[5] Huang K T, Cohen R M and Stringfellow G B 1995 *J. Cryst. Growth* **156** 320
[6] Kajikawa Y, Asahina S and Kanayama N 2001 *Japan. J. Appl. Phys.* I **40** 28
[7] Yamamoto K, Asahi H, Fushida M, Iwata K and Gonda S 1997 *J. Appl. Phys.* **81** 1704
[8] Asahi H, Koh H, Takenaka K, Asami K, Oe K and Gonda S 1999 *J. Cryst. Growth* **201/202** 1069
[9] Storm D F, Lange M D and Cole T L 1999 *J. Appl. Phys.* **85** 6838
[10] Kajikawa Y, Asahina S and Kanayama N 2001 *Japan. J. Appl. Phys.* I **40** 28
[11] Kajikawa Y, Kubota H, Asahina S and Kanayama N 2002 *J. Cryst. Growth* **237/239** 1495
[12] Kajikawa Y, Kobayashi N and Kanayama N 2003 *J. Appl. Phys.* **93** 2752
[13] Blaha P, Schwarz K and Luitz J 1997 *WIEN2k* University of Technology, Vienna
This is an improved and updated Unix version of the original copyrighted WIEN code, which was published by
Blaha P, Schwarz K, Sorantin P and Trickey S B 1990 *Comput. Phys. Commun.* **59** 399
[14] Perdew J P, Burke K and Ernzerhof M 1996 *Phys. Rev. Lett.* **77** 3865
[15] Monkhorst H J and Park J D 1976 *Phys. Rev.* B **13** 5188
[16] Murnaghan F D 1944 *Proc. Natl Acad. Sci. USA* **30** 244
[17] Ferreira da Silva A, Souza Dantas N, de Almeida J S, Ahuja R and Persson C 2005 *J. Cryst. Growth* **281** 151

[18] Wang S Q and Ye H Q 2002 *Phys. Rev.* B **66** 235111
[19] Mankefors S and Svensson S P 2000 *J. Phys.: Condens. Matter* **12** 1223
[20] Ferhat M and Zaoui A 2006 *Phys. Rev.* B **73** 115107
[21] Villars P and Calvert L D (ed) 1985 *Pearson's Handbook of Crystallographic Data for Intermetallic Phases* (Metals Park, OH: American Society for Metals)
[22] Ferhat M and Zaoui A 2006 *Appl. Phys. Lett.* **88** 161902
[23] Vurgaftman I, Meyer J R and Ram-Mohan L R 2001 *J. Appl. Phys.* **89** 5815
[24] Pearsson C and Zunger A 2003 *Phys. Rev.* B **68** 073205